Simulations of Current Coupling in Ion Beam-Neutralizer Interactions

Adrian Wheelock, David L. Cooke
Air Force Research Laboratory, Space Vehicles Directorate
29 Randolph Road, Hanscom AFB, MA USA 01731-3010 (FAX: 781-377-2491)

Nikolaos A. Gatsonis
Worcester Polytechnic Institute, Mechanical Engineering Department
100 Institute Road, Worcester MA USA 01608 (FAX: 508-831-5680)

Abstract

Neutralization of ion beams in electric propulsion applications is a well-known phenomenon. The physics behind the robust matching of ion and electron currents and densities, are not. As electric propulsion devices move into micro and macro regimes with colloids, FEEPs, and thruster arrays, thruster-neutralizer interactions are under increasing scrutiny. A series of 2D simulations using PIC codes are presented, detailing starting and steady state interactions. It is shown that the expectations of full current coupling of electrons to the beam is not seen, but there is similar coupling behavior exhibited. Numerical mechanisms for coupling the current to the beam are examined for effect on coupling behavior.

Introduction

Ion beam neutralization during operation of electric propulsion devices requires both current and charge density matching with an emitted electron beam. This current coupling is easily accomplished in reality, yet the exact process remains unknown. Currently the neutralization process is described through an "effective collision frequency" that binds electrons to the ion beam. As electric propulsion becomes more prevalent in space missions, this question garners significant importance. Proper modeling of current coupling and neutralization will enable development of low-current neutralizers and optimization of neutralizers for micropropulsion devices. Explanation of the effective collision frequency also has bearing on space instrument calibration, electrodynamic tethers, and ionospheric research.

In the early years of electric propulsion research, the neutralization question was one of the fundamental issues for successful development of this promising technology. A dense ion beam requires space charge neutralization to avoid a potential barrier that can divert or reflect the beam. The vehicle on which the thruster operates needs current neutrality to avoid unwanted charging. In the context of collisionless plasma theory, achieving both current and charge neutrality with the same source of electrons appears to be nearly impossible owing mostly to the large difference in mass between electrons and the ions. For example, define the ion flux, $F_i = N_i v_i$, and the net electron flux, $F_e = \frac{1}{4} N_e v_{eth}$, where N is density, v is velocity, i and e are ion and electron subscripts and eth designates the electron thermal velocity for an idealized electron source. Equal density and flux requires $v_{eth} = 4v_i$. A 1 keV Xenon beam has v_i=38,000 *m/s* so a matching electron velocity requires a source temperature of about 0.05 eV. A challenging, but not impossible number, but a collisionless analysis suggests that detailed balancing is required, whereas real systems quite easily achieve 'beam coupling.' Of course a higher temperature, lower density electron source will lead to a positive potential well that does trap electrons, but then the theory must explain by what process the trapped electrons shed energy so as to actually fill the well. Another observation, presented in more detail below, is that when ion beams and neutralizers are operated in conducting vacuum tanks, the currents are closely coupled even though the grounding tank eliminates the charge accumulation that could provide feedback for current balance so it appears that one or more plasma mechanisms must be responsible for this collective phenomena -- charge and current neutrality – which we hereafter call current coupling.

Our immediate goal is to determine if what might be considered standard Particle-In-Cell, PIC, techniques are adequate or if additional treatment is needed to understand and capture the beam coupling

process. In this paper we present first a review of neutralization studies. We then present a series of simulations using a 2-D PIC code[1] as well as the implementation of a 3D PIC/DSMC code.[2,3] These show the dependence of the beam neutralization on beam energy and neutralization current. The simulations presented in this paper serve also as means of validation of the PIC-modules of our PIC/DSMC code under development.

History of EP Neutralization

Possibly first pointed out by L. Spitzer in 1952 [uncited note in Seitz et al. 1961][4], electric propulsion plumes needed to be properly mixed with electrons or else severe space-charge effects would result. Before the first space tests, serious doubts lingered as to the stability of any neutralization approach to the ion beam created by an electrostatic thruster. The general idea was for neutralization to occur shortly after emission to prevent beam return. However, a lack of understanding as to how the electrons would stay within the beam if injected or even if the neutralization process was unstable to small perturbations brought about significant research activity. Failing to properly neutralize the beam would cause a dramatic reduction in thrust, as a significant portion of the beam would return to the spacecraft. This problem was first addressed by the Ramo-Wooldridge staff in their review of electrostatic propulsion in 1960.[5] Their one-dimensional investigation was admittedly unrealistic enough to provide a satisfactory indication as to the stability and practicality of neutralization.

Over the next few years, many theorists who looked at 1- and 2-D models predicted growing instabilities that could turn the beam back to the spacecraft. Some research pointed towards the possibility of neutralization, such as French[6] and Mirels. (1961)[7] Other work pointed towards potential problems, such as Seitz et al. Some of the earliest computational studies were brought to bear on the problem, and Buneman and Kooyers[8], using a one-dimensional code in 1963, were able to provide a neutralized beam when electrons were injected at energies lower than the directed ion energy and velocities on the same order. Fluctuations in the space charge field provided mixing of the beam. Two years later Wadhwa et al.[9] performed a two-dimensional PIC simulation showing that electrons would oscillate within the beam to allow for neutralization, but theorized the oscillations were not the only mechanism at work. One method suggested was that fluctuations in the space-charge field allowed for entropy increase to mix the electrons, but these fluctuations were not found far downstream of the neutralizer, suggesting a collective cooling mechanism. Work thus far looked only at space charge neutralization, not current neutralization.

The 1964 Space Electric Rocket Test I (SERT I) found that it was quite easy to neutralize ion beams in space using straightforward neutralizer geometry. In a series of tests it was shown that the ion thruster developed thrust at a level indicating complete beam neutralization. This indicated that the ion and electron velocities were matching so that current coupling was happening without impact on vehicle potential or thrust produced. After SERT I, proof of concept was achieved and the theoretical discussion of beam neutralization was dropped in favor of engineering new thrusters. Studies after SERT I include evaluations of neutralizer placement[10,11], optimization of the thrusters, and simulations to analyze spacecraft-plume interactions.[12,13] A few numerical simulations of neutralization have been performed recently, including Othmer et al.[14,15,16] using a relativistic 3D PIC simulation and Tajmar and Wang investigating FEEP neutralizer placement.[10] Othmer suggested that electrons reflected from the ends of the beam therefore eventually matching velocities, but this does not explain why current coupling can be observed in a vacuum chamber, where the beam is nominally stationary and bounded. Tajmar was not investigating the coupling effect directly. Work in the nuclear fusion community has recently[17] investigated pulsed plasma beams being neutralized by background plasma, but the high powers and densities involved make a direct connection difficult.

Despite decades of research and the implementation of electric propulsion devices, the detailed process by which an ionized beam is neutralized in space is still unknown. Assorted methods to fit data with theory have been found, but the actual process has yet to be studied in sufficient detail to fully understand the subject. Further, new electric micropropulsion devices such as the FEEP or the colloidal thrusters or large arrays of ion and Hall thrusters are still not guaranteed to behave. We might also desire a means to predict and optimize neutralizer operations. Thus, a simulation technique exhibiting beam coupling is needed. Additionally, results from ion beam neutralization modeling will be applicable to ion beams for instrument calibration, electrodynamic tethers, ionospheric research, and fundamental plasma physics.

Current Coupling Observations in a Vacuum Tank

In order to observe this phenomenon directly, we utilized the JUMBO large vacuum facility (2 meter diameter) at AFRL/Hanscom. A 3-cm IonTech ion source, functionally identical to an electrostatic

ion engine, was installed. This source used a hot tungsten wire placed across the beam to provide neutralization, although in a vacuum tank it is not required for operation due to neutralization at the conducitng wall. The ion source was able to run on a wide variety of gases; for these tests we used nitrogen.

Table 1: Ion Source Settings

Cathode Current	3.00 A
Discharge Voltage	55.0 V
Accelerator/Beam Current Limit	20 %
Background Pressure	5E-4 Torr

The controller enabled accurate control of beam (extractor) voltage to 1V, neutralizer filament current to 10mA and measurement of beam (extracted) current and neutralizer emission current to an accuracy of 1mA. With other settings shown in Table 1, three tests were performed, one with the beam voltage set to zero, one at 450 V and one at 800 V. In each test, the heater current was increased from zero to 3.50 A, a level sufficient for saturation of the emitted current, then brought back to zero. The results can be seen in Fig. 1, 2, and 3.

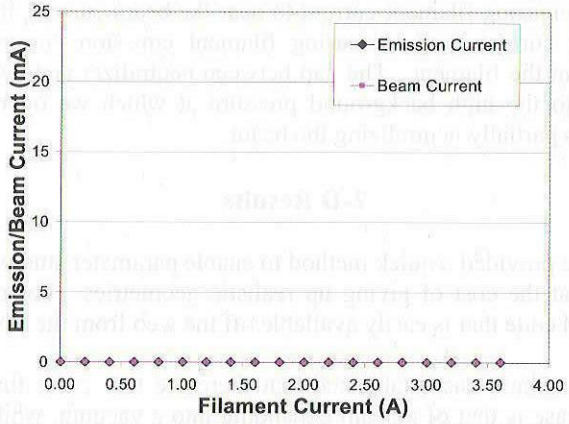

Figure 1: Currents with no ion beam

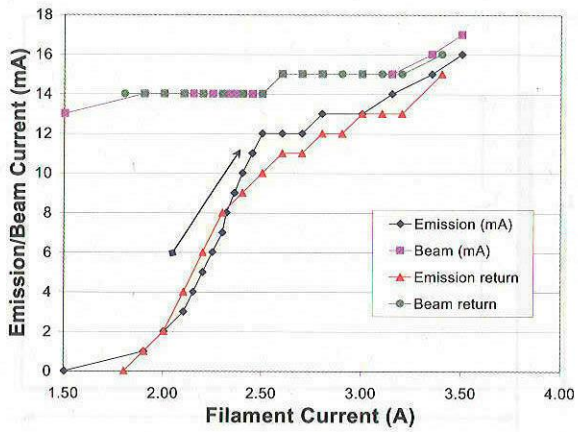

Figure 2: Currents with 450V ion beam

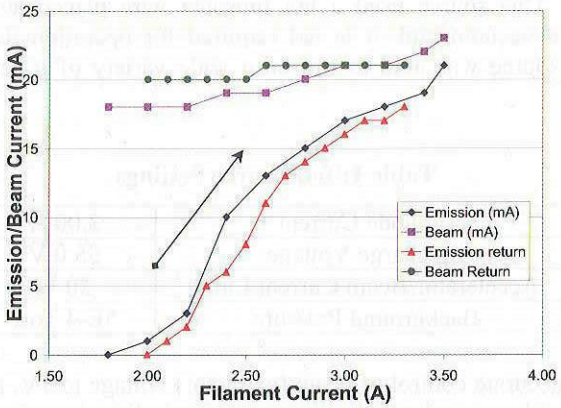

Figure 3: Currents with 800V ion beam

As expected, without an ion beam present, even though the filament current was at over 3 A, the filament emission current saturated at less than 0.1mA. Once a beam was provided, however, the emission current quickly rose with increasing filament current to near the beam current, though never quite reached it. The increase in beam current with increasing filament emission current we theorize is due to backstreaming electrons from the filament. The gap between neutralizer and beam current may be due to charge-exchange ions due to the high background pressure at which we operated as well as electrons released from chamber walls partially neutralizing the beam.

2-D Results

Simulations in 2-D have provided a quick method to enable parameter studies without the complexities and hassle of a 3-D code, at the cost of giving up realistic geometries. For our studies, we have used XOOPIC, an object-oriented code that is easily available off the web from the Berkeley Plasma Theory and Simulation Group.

Previous work by the authors has established that there are two cases that XOOPIC is capable of performing. The "filling" case is that of a beam expanding into a vacuum, while the "chamber" case is a beam propagating across a bounded domain that is grounded. Since current coupling can be observed in a chamber, as demonstrated above, we focus on the "chamber" case. Discussion of the filling case can be found in Wheelock et al.[18],[19]

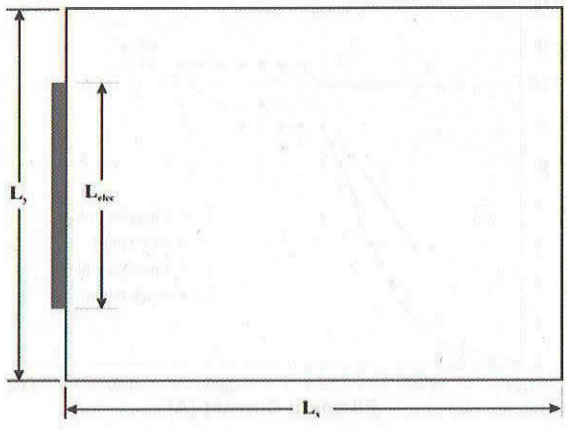

Figure 4: 2D simulation domain

In the chamber case, if current coupling is modeled by standard PIC, then there should be a preference for electron flow in the direction of ion flow. Utilizing the ability of computer code to

manipulate the ions, we can determine if there is an effect of ion motion or numerical parameters on the electrons. The easiest way to measure this is through the particle flux through either side. If a bias exists that is created by ion motion, it would be evident by comparing the number of electrons leaving each side. Electrons are injected from each end to avoid any bias in the collected current created by ballistic electrons.

A manipulation available only in simulation is the "freezing" and "unfreezing" of ions through use of ion subcycling. By doing this we can isolate ion motion effects. A quick comparison of two simulations using otherwise identical 1keV Xenon ion beams, one frozen, one with mobile ions, creates a slight difference in the flux of electrons through each side, on the order of 5%. A beam with frozen ions has matching fluxes out either end. To further examine this, we took a beam with frozen ions and allowed it to subcycle once during a simulation. The ions and electrons were loaded with a cold quiet start, so before the ions move, there is zero motion in the simulation as seen in **Figure 5**. After the ions cycle, the electrons are set in motion with the same 5% bias to the downstream side by induced fluctuations in the electric field. This shows some coupling is observed, but the question becomes, "Is this what is expected in PIC?"

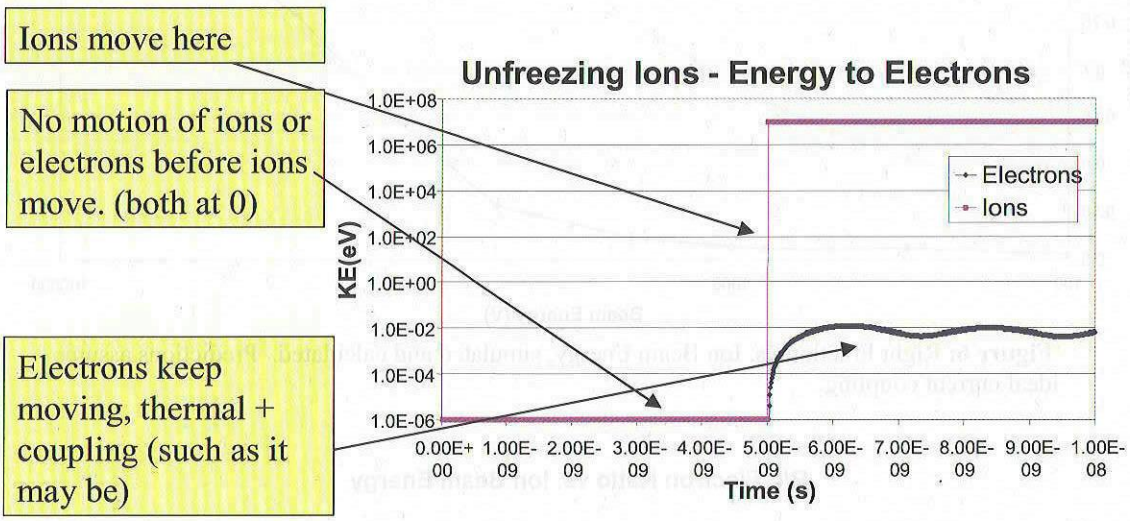

Figure 5: Ion/Electron energy before/after ion timestep.

To answer this question, we begin by looking at the drifting 1-D Boltzmann-Maxwell distribution function. For now, we assume that the drift is caused by a complete coupling of the electrons to the beam, indicating $v_{drift} = v_{beam}$.

$$f_e(c) = \left(\frac{m_e}{2\pi kT}\right)^{\frac{1}{2}} \exp\left(-\frac{m_e (c-u)^2}{2kT}\right) \tag{1}$$

Multiplying by the thermal velocity and integrating over the halves of velocity space gives us the flux either in the direction of the drift (beam), or opposite it.

$$\int_0^\infty c f_e(c)\, dc = -\frac{1}{2}\left(\frac{a}{\pi}\right)^{1/2} \left(\sqrt{a} + u\sqrt{\pi}\,\mathrm{erf}\left(\sqrt{a}u\right) a \exp\left(au^2\right) + u\sqrt{\pi} a \exp\left(au^2\right)\right) \Big/ a^{3/2} \exp\left(au^2\right) \tag{2}$$

where $a = m_e/2\pi kT$.

Comparison of this result to the fluxes generated by XOOPIC can provide a basis for comparison of the observed coupling compared to expected coupling. This analysis provides expected electron motion

based on the beam energy, which is easily tested in simulation. Figure 6 shows the simulated and projected flux ratios and Figure 7 shows the fraction of electrons exiting through the downstream side. As can be clearly seen, the simulations provide the same basic behavior, but at a drastically reduced rate. This may indicate incomplete coupling or a numerical effect based on a gridded electrostatic potential.

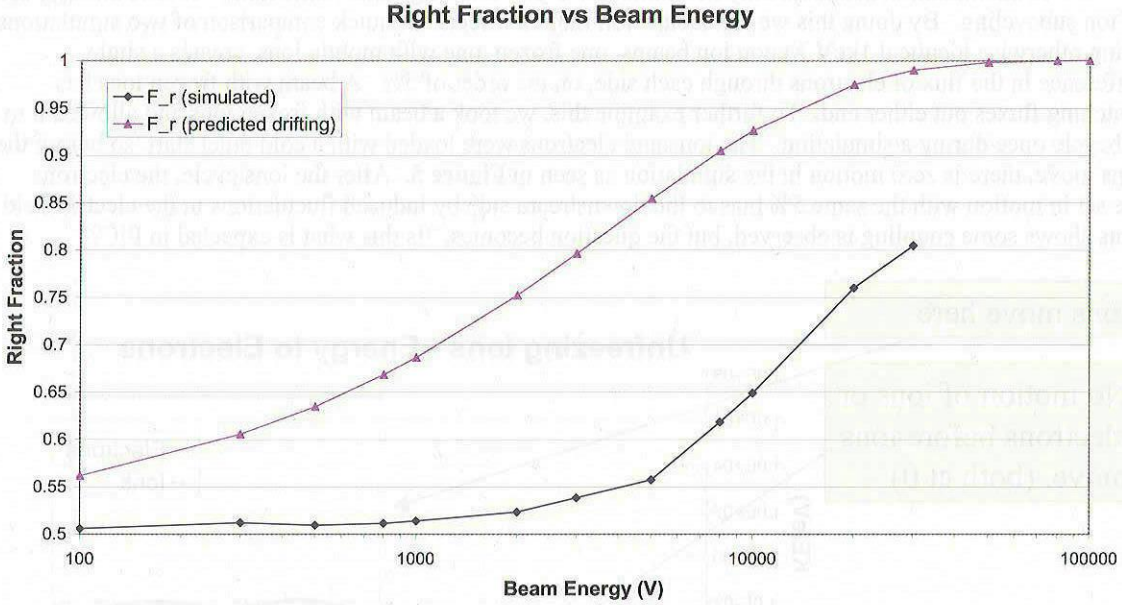

Figure 6: Right Fraction vs. Ion Beam Energy, simulated and calculated. Predictions assume ideal current coupling.

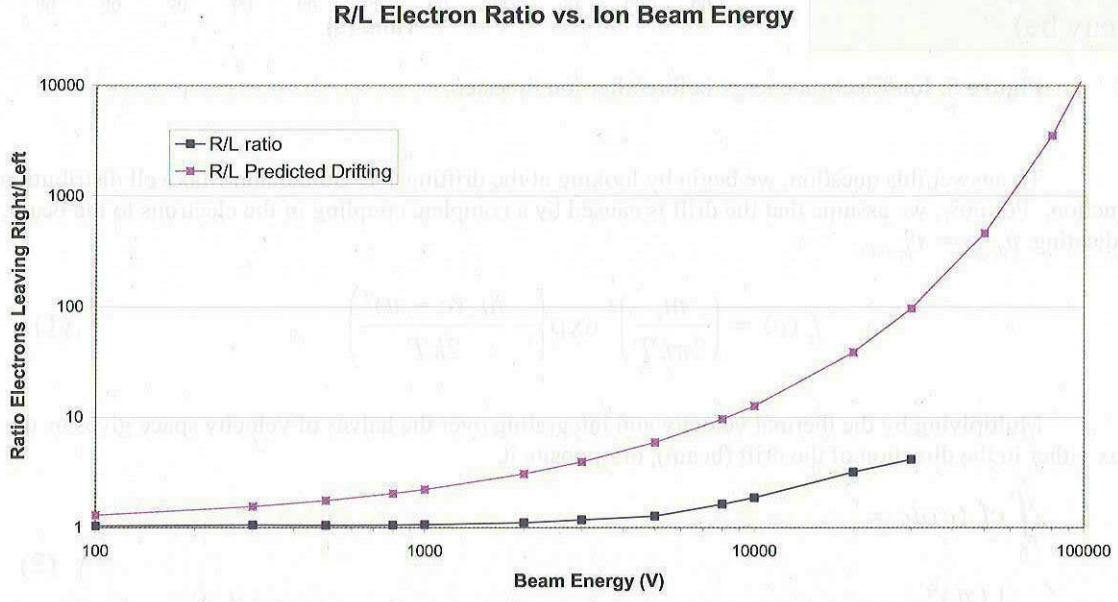

Figure 7: Electron Ratio vs. Ion Beam Energy, simulated and calculated. Predictions assume ideal current coupling.

To eliminate possible numerical effects, a series of parameter studies was conducted, examining the effects of duration of simulation, particle weighting, cell size, and length of the simulation domain. While these do show some variation, the effects mostly point to modes of the problem rather than distinct numerical effects.

Varying the particles per cell does not seem to have an appreciable effect at either 100eV or 1keV ion beam energies as seen in Figure 8. Some potential modes are presented, but none that significantly affect the coupling observed. A similar effect is seen in Figure 9, where modes are visible but the duration of the simulation only seems to enhance the low-energy ions. Figure 10 shows the effect of domain size on the simulation, again with no significant variation in coupling rate.

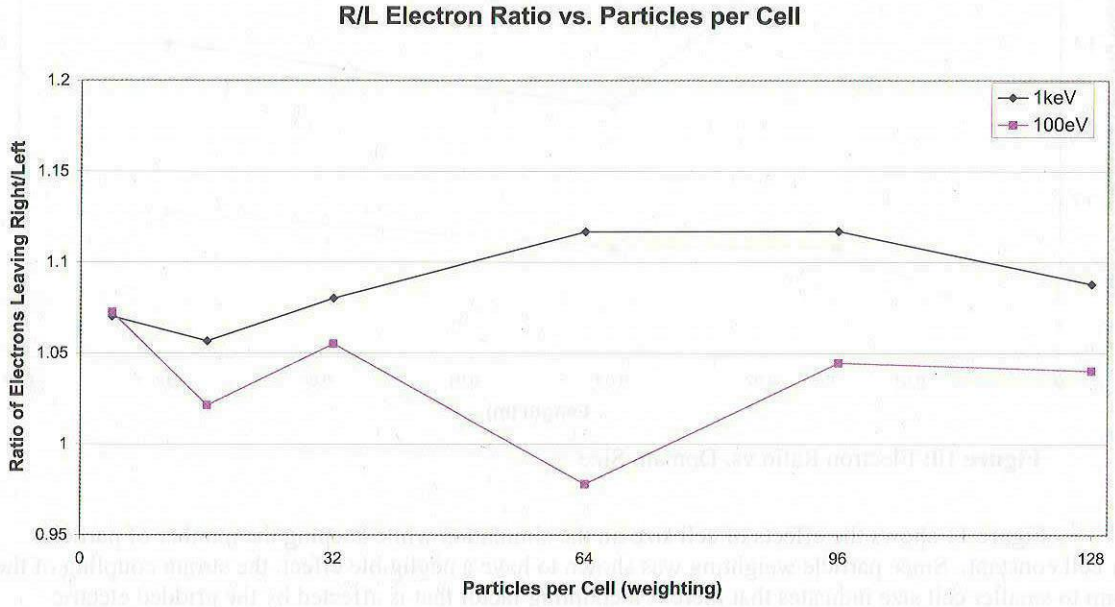

Figure 8: Weighting effects on electron ratio.

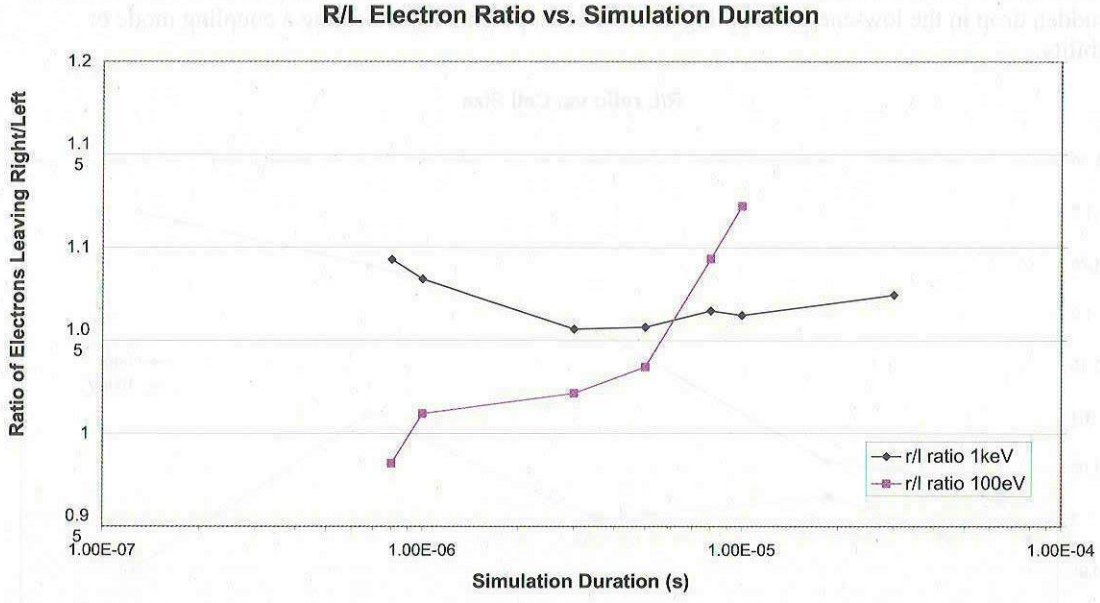

Figure 9: Electron Ratio vs Simulation Duration

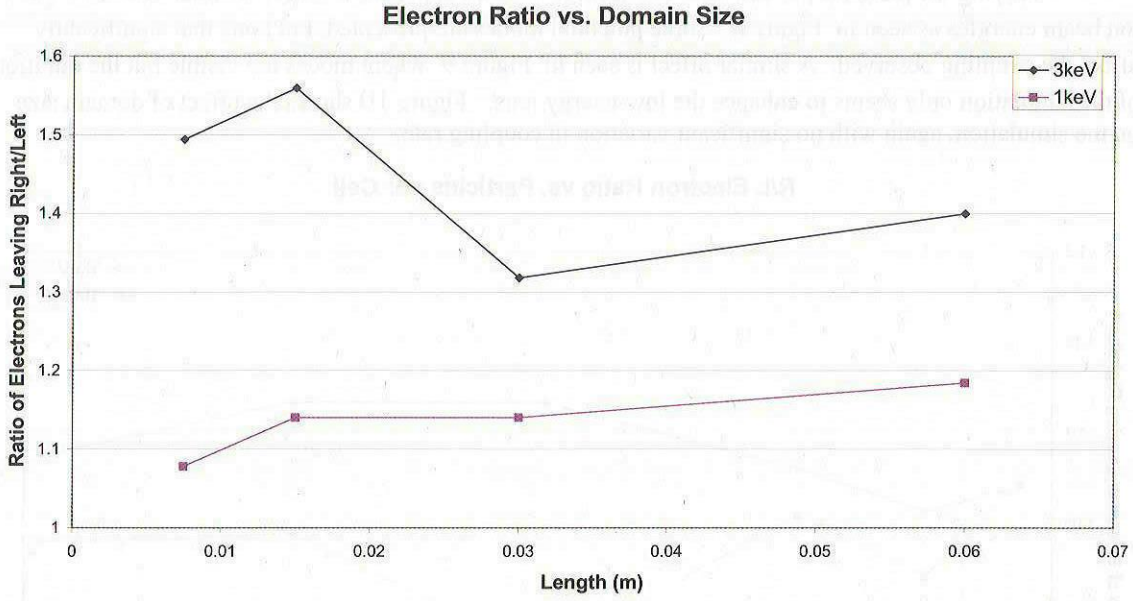

Figure 10: Electron Ratio vs. Domain Size

Figure 11 shows the effects of cell size on the simulation while keeping the number of particles per cell constant. Since particle weighting was shown to have a negligible effect, the strong coupling of the beam to smaller cell size indicates that there is a coupling factor that is affected by the gridded electric field. Whether this is due to enhanced fluctuations by creating more cell boundary crossings and therefore disrupting the phase-space population in each cell or through reweighting of ion charge to the grid, the ion motion is still minimal, with at most a handful of crossings each timestep. An alternate explanation could center around better resolution of coulomb collisions and increased particle interaction. A curious note is the sudden drop in the low-energy coupling at 1024 cells, potentially indicating a coupling mode or instability.

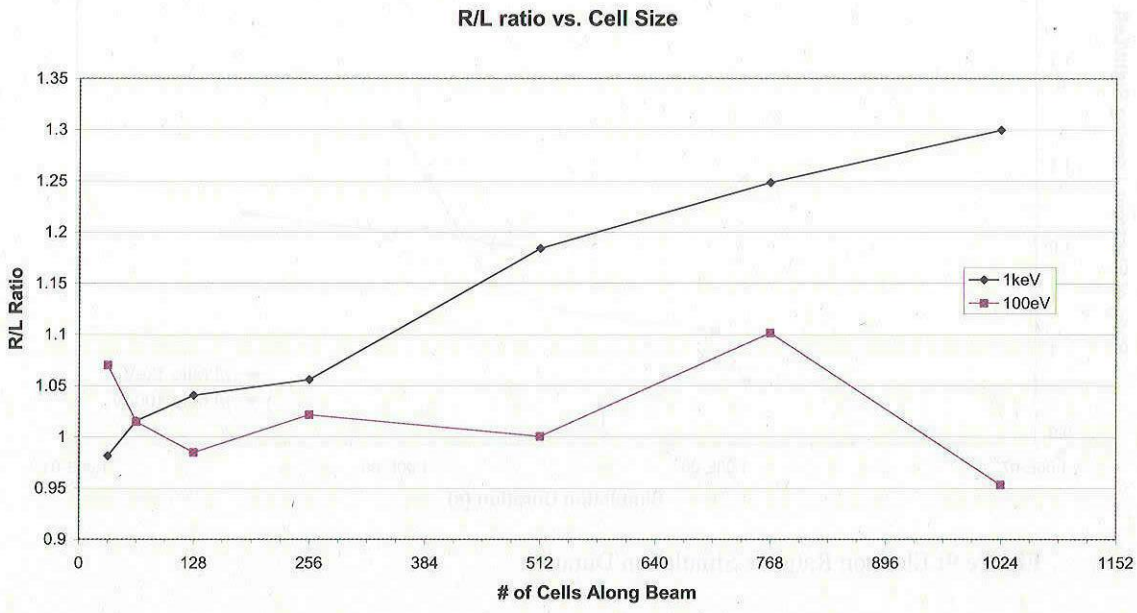

Figure 11: Electron Ratio vs. Cell Size

2D Discussion

While it is clear that there is some coupling observed in the simulations, it does not correspond to the calculated effects of full coupling as described above. By examining the simulated ratios, we can come to the conclusion that if some fraction of the beam is coupling, $f_c=n_c/n_0$, the ratio of the simulated curve to that predicted by full coupling would scale as

$$\frac{n_c}{n_0} = f_c = \frac{f_{r,simulated} - 1/2}{f_{r,predicted} - 1/2} \tag{3}$$

This examination leads us to the rough estimate that we are seeing 5-15% of the electrons coupling with the ion beam across most of the energy range investigated, with greater coupling as the ions increase in energy.

Still unanswered is the question as to the method by which the electrons are being accelerated along the beam. Several possibilities come quickly to mind, including velocity drag and the two-stream instability.

Looking at the velocity drag relations for a 1D problem as described in Birdsall, we can easily extrapolate to a 2D or 3D situation. As given by Birdsall, the acceleration felt by a particle in 1D is

$$\frac{dv}{dt} = -\frac{\omega_p v_t}{2N_D} = -\frac{q^2}{2m} \tag{4}$$

This can easily be shown in 2D to be

$$\frac{dv_x}{dt} = -\frac{q^2\theta}{\pi m} \tag{5}$$

Where $\theta = \arctan v_t/v_{x,i}$. This is due to the shock cone behind the particle moving at superthermal velocities through the background plasma with information of its passing spreading perpendicular to its direction of travel only at the thermal velocity v_t. In the limit of infinite v_t, this reduces to the 1D acceleration. This acceleration is constant, so we can quickly examine its effects. With realistic q, m, v_t, and 1kV ions, it is quickly shown that the acceleration time for electrons to match ion speeds in this case is on the order of years for v_t comparable to that observed (~0.3eV). Indeed, the 1D case shows a heavy bias towards higher thermal temperatures.

Examination of the two-stream instability shows that any counterstreaming beams are unstable at certain wavelengths. The growth rate of the ion/electron two-stream instability is known to be

$$\gamma = \omega_p \left(\frac{m}{M}\right)^{\frac{1}{3}}. \tag{6}$$

This growth rate still fails to provide significant coupling as the time for the oscillation to grow is strongly limited by the electron-ion mass ratio. Again using the constant acceleration formulas, significant fractions of a second are required for the instability to grow to nontrivial levels, far beyond the duration of the simulations performed. Growth rates this small would take the beam mixing point far beyond the area of interest to any spacecraft.

The elimination of these effects retains the conundrum that we have laid out for ourselves, namely the determination of the mechanism through which an electron beam will couple in both current and space charge with an ion beam. While some coupling is observed in PIC simulations, the mechanism for the coupling remains unknown.

Unstructured 3D PIC Code Description

While the majority of our simulations were performed using the code XOOPIC, we have also begun using our 3D PIC/DSMC code[2,3] to examine the problem in a more realistic fashion. We have developed an unstructured grid generator that provides three-dimensional meshes of arbitrary geometry and allows for adaptation of the mesh according to the preliminary solution obtained on an initial grid. The generator is based on Watson's[20] incremental node insertion method, using properties of Delaunay[21] triangulation.

The general procedures for loading and injection used follow Birdsall et al.[22] and Bird.[23]

Integration of the equations of motion of a charged particle are performed by the Boris method[24] as discussed by Birdsall et al.[27] Particles are moved between adjacent cells using a particle-tracing technique.

To formulate a finite volume method for Poisson's equation

$$\nabla^2\Phi = -\frac{\rho}{\varepsilon_o} = -\frac{\sum_{i=1}^{Ni} q_i n_i + q_e n_e}{\varepsilon_o} \tag{7}$$

advantage is taken of the Voronoi dual of the Delaunay triangulation to associate an irregular volume to each node on the grid. The Voronoi cell corresponding to each Delaunay node contains the set off points closer to that node than any other, the facets of the Voronoi cell are orthogonal to the lines joining the tetrahedral nodes as shown in Figure 4.

This method reduces Gauss' law for a node-centered finite volume scheme to the standard 2nd order finite-difference method on Cartesian meshes.

In a bounded domain, piece-wise Dirichlet and Neumann boundary conditions specify a solution of Poisson's equation. Since the boundaries of the Delaunay mesh are forced to coincide with the boundaries of the computational domain, boundary condition implementation is straightforward. In the case of a Dirichlet boundary condition, the voltage is placed on the right hand side of the matrix and the corresponding row is zeroed, with a one placed on the diagonal. Fluxes in Neumann boundary conditions are added to the flux formulation for the Voronoi cell corresponding to the boundary node, with the value of the inward normal electric field multiplied by the boundary area added to the right hand side of the node of interest.

In matrix form with boundary conditions as in Figure 3, Gauss' law is:

$$\begin{bmatrix} 1 & 0 & 0 & \cdots & 0 \\ R_{2,1} & R_{2,2} & R_{2,3} & \cdots & R_{2,N} \\ R_{3,1} & R_{3,2} & R_{3,3} & \cdots & R_{3,N} \\ \vdots & \vdots & \vdots & \ddots & \vdots \\ R_{N,1} & R_{N,2} & R_{N,3} & \cdots & R_{N,N} \end{bmatrix} \begin{Bmatrix} \Phi_1 \\ \Phi_2 \\ \Phi_3 \\ \vdots \\ \Phi_N \end{Bmatrix} = \frac{1}{\varepsilon_o} \begin{Bmatrix} Q_1 \\ Q_2 + \varepsilon_0 E_{N,2} A_{N,2} \\ Q_3 \\ \vdots \\ Q_N \end{Bmatrix} \tag{8}$$

N is the number of nodes in the mesh. The coefficients are determined by

$$\begin{aligned} R_{i,j} &= \sum_{k=1}^{N_{F,i}} \frac{A_{i,k}}{L_{i,k}} \text{ for } i = j, \\ R_{i,j} &= -\frac{A_{i,j}}{L_{i,j}} \text{ if } j \text{ is adjacent to } i, \\ R_{i,j} &= 0 \text{ otherwise} \end{aligned} \tag{9}$$

$A_{i,j}/L_{i,j}$ is the ratio of the area of the Voronoi face A_{ij} between nodes i and j to the distance between nodes i and j if the nodes $L_{i,j}$. The boundary conditions for node 1 are Dirichlet with potential Φ_0, and node 2 is on a Neumann boundary with inward flux $E_{N,2}A_{N,2}$.

Gauss' law may now be solved by a variety of linear solvers. Our current method uses Jacobi iteration to provide a solution, but this method is quite slow for computationally large problems. Also, the size of the domain we are interested in requires large numbers of particles in a high-resolution mesh, further slowing the computation.

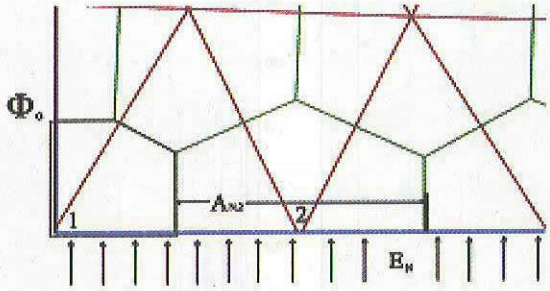

Figure 12: Boundary Conditions on Voronoi Dual.

To remedy this issue, we have begun investigating parallelizing the code using OpenMP and PETSc[25]. The modular functionality of PETSc allowed us to parallelize only the Poisson solver subroutine without drastic modifications to the rest of the code. We are presently evaluating if conversion to PETSc or a self-programmed MPI interface is preferable. If, upon evaluation, PETSc is a method we are comfortable with, the parallelization will expand to more of the code until it is a fully parallel program. An alternate parallelization method is simply the creation of a special boundary condition.

As in many math libraries, the careful construction of matrices and vectors is key to utilizing the solvers the library provides. To ensure a standard interface to its solvers, PETSc has native data structures for vectors and matrices, which automatically handle parallel data distribution. Data was required to be translated between Fortran90 vectors and PETSc data structures. These vectors were distributed across the processes, with lower-ranked processes getting any extra rows. Once the data structures were built, they were passed on to the Krylov solver. GMRES[26] was selected from a provided suite of Krylov Subspace solvers using a Jacobi preconditioner.

OpenMP was inserted in a variety of simple loops where it would enhance performance. Due to overhead, it may or may not speed up execution. For cases where it would not enhance performance, a compile-time flag can be commented out of the makefile to turn off OpenMP. OpenMP was active for the test case. To validate the parallel code, a simple test case was run for 200 timesteps on a 2x8 Linux cluster and the results compared, as seen in Figure 13. The results were effectively identical.

Unfortunately, the overhead of the parallelism was unable to speed up the test case. As shown in Figure 14, the time to perform the test case increased as the number of processors increased. It is likely, however, that these numbers can be improved in larger domains and as more of the code begins to use PETSc, so time is not wasted transferring data between PETSc and the rest of the code.

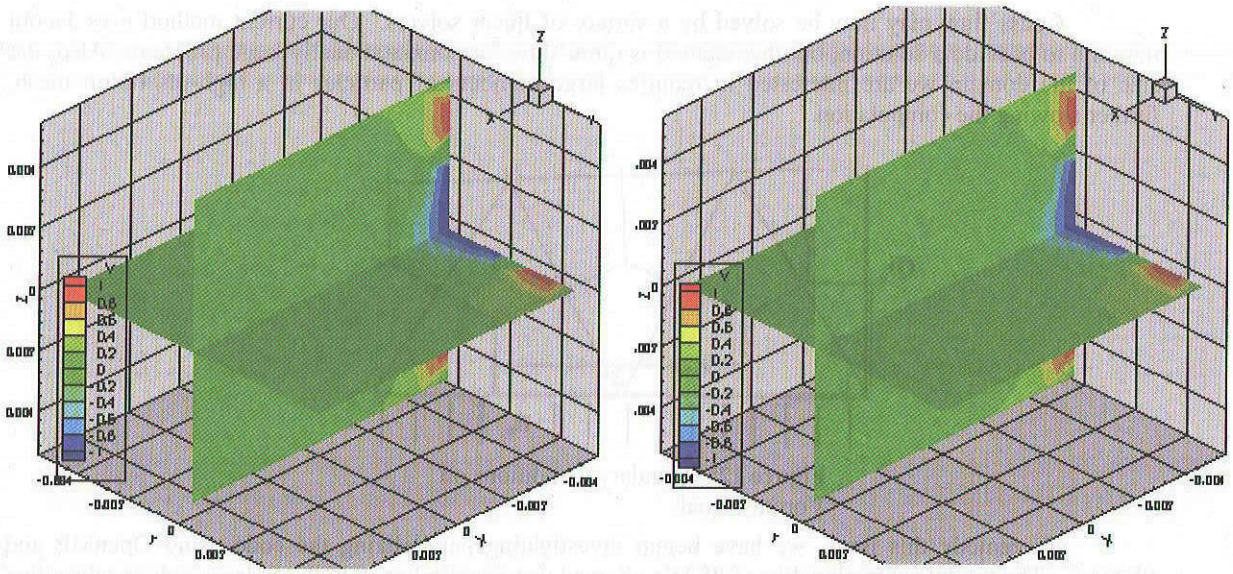

Figure 13: Comparison of ion beam inside annular electron beam at 200 timesteps. Left: GMRES/PETSc Right: Unmodified Jacobi Iteration

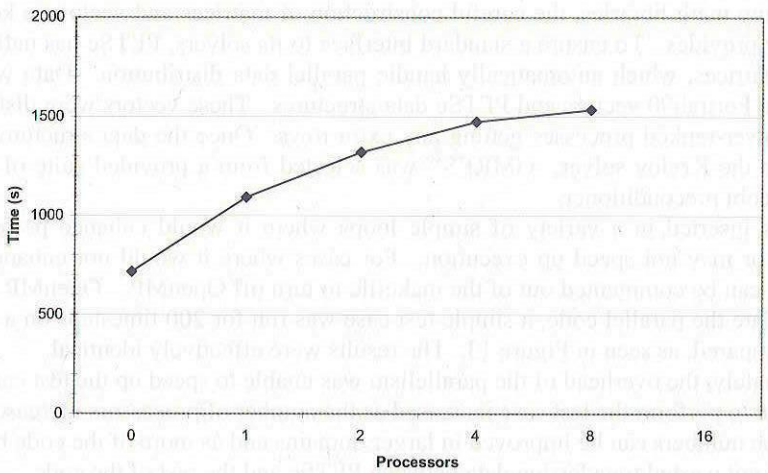

Figure 14: Speedup (Slowdown) of 3-D code. 0 is unmodified case with all speedups activated.

3-D Results

To perform unstructured 3-D simulations with realistic mass ratios requires quite a bit of computational time. The majority of the efforts in this area went into parallelizing the code and attempting to improve the mesh generator.

The 3-D simulation domain is shown in Figure 15. The cylindrical domain of radius R and length L consists of a circular emission area with radius r where both ions are injected. Around this is an annular emission region of inner radius r2 outer radius r3 where electrons are emitted. While this is unphysical, this easily examined the ability of electrons to move into an ion beam. Future work will include a separate neutralizer.

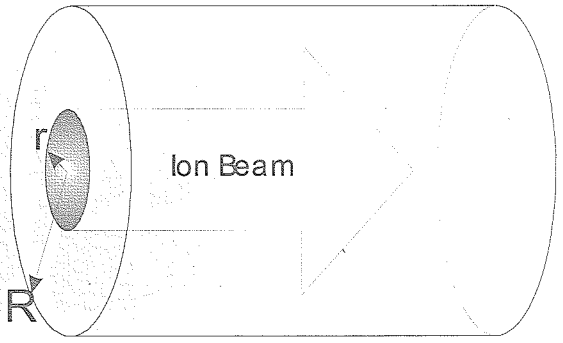

Figure 15: 3-D Simulation Domain

Due to the longer simulation time required of 3-D runs, only a few simulations were performed for the present work. A domain with $L = R = 0.01$ m was generated with beam injection surface radius $r = 0.002$ m and the electron injection surface between $r_2 = 0.003$ m and $r_3 = 0.004$ m. The background was held at a density of 1E11 while the injected density was 1E15 for both ions and electrons in the first run, and was 5.7E14 for electrons in the second run to match emitted currents. Injected velocity was set to 12122.5 m/s to correspond to a 100eV Xenon beam and 41935.9 m/s to correspond to a 0.01eV electron beam. Injected temperatures were held at 0.1 eV for both ions and electrons. Surfaces on the injector side were set to be solid conductors while the downstream surfaces were free space, allowing particles to exit the simulation.
It can be seen in Figure 16 that a well forms in the ion beam, drawing the electrons in to maintain quasineutrality. The beam then propagates across the simulation domain, drawing electrons with it.

Conclusions

We have shown that PIC models some behavior similar to the current coupling observed in electric propulsion devices. We have developed a theory for the expected behavior, but the discrepancy in simulation and theory is significant, although the general behavior is correct. Using the 2-D PIC code XOOPIC, we have determined that the degree of coupling depends primarily on the energy of the ion beam. Numerical effects such as particle weighting, simulation duration, and domain size were found to be of no significant effect on the observed coupling. Cell size did play a noticeable role, indicating some dependence on the granularity of the simulation.

Physical effects that could cause a mixing of the beams or an acceleration of the electrons were examined and found insufficient to produce the simulated effect. Until it can be adequately explained what processes allow current coupling, neutralization will remain a feature that cannot be engineered for. Previous research has not pointed out an adequate explanation for this effect.

To allow exploration of three dimensional effects and problems with sizes of engineering interest, we are developing a parallel 3D code. As simulations progress to more realistic geometries, perhaps more insight can be gained for application to placement and design of neutralizers.

A series of laboratory experiments capable of reproducing the simulations is necessary to understand the actual dynamics of the system. With experimental data, theory can be refined to a point where calculations of engineering use are possible.

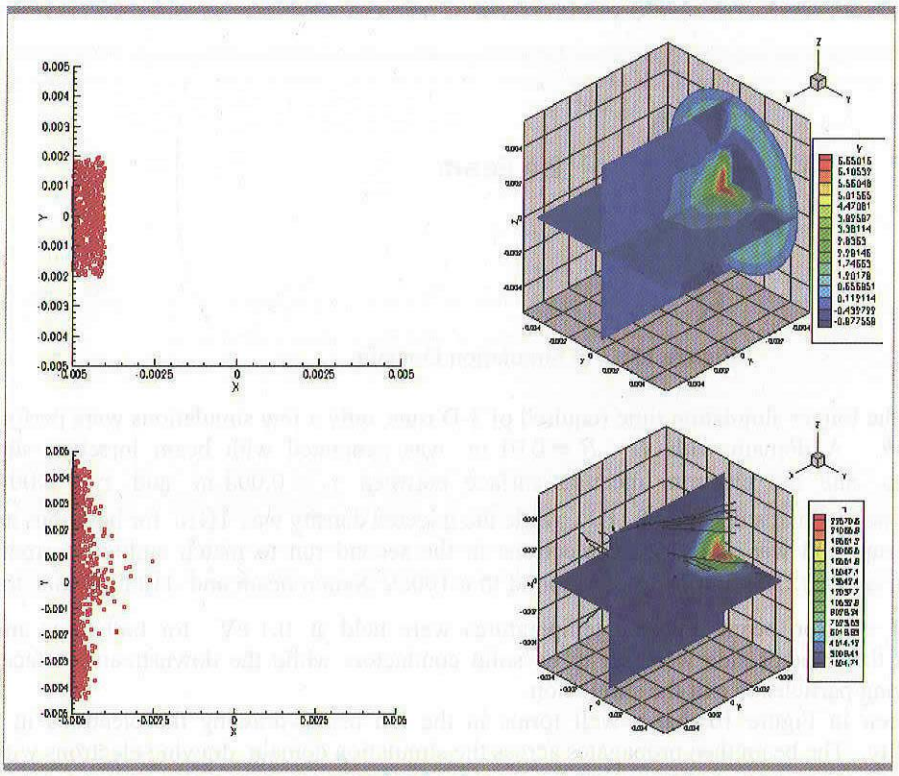

Figure 16: 3-D Simulation results. Left: X-Y phase space for ions (top) and electrons (bottom). Right Top: Potential Right Bottom: Temperature and velocity streaklines.

References

[1] Verboncoeur, J.P., Langdon, A.B. and Gladd, N.T. "An Object-Oriented Electromagnetic PIC Code," *Comp. Physics Comm.*, 87, pp. 199-211, May 1995.

[2] Gatsonis, N.A. and Spirkin, A. "Unstructured 3D PIC Simulations of Field Emission Array Cathodes for Micropropulsion Applications." 38th Joint Propulsion Conference, Indianapolis, IN, July 7-10 2002.

[3] Spirkin, A. and Gatsonis, N.A. Unstructured 3D PIC Simulation of Plasma Flow in a Segmented Microchannel. 36th AIAA Thermophysics Conference, Orlando, FL, June 23-26 2003.

[4] Seitz, R.N. et al. "Present Status of the Beam Neutralization Problem." *Progress in Astronautics and Rocketry Volume 5: Electrostatic Propulsion*, p.383-422, Academic Press, New York, 1961.

[5] Ramo-Wooldridge Staff. "Electrostatic Propulsion." Proceedings of the IRE, Vol. 48, No. 4, April 1960.

[6] French, Park. "Circular Beam Neutralization." *Progress in Astronautics and Rocketry Volume 5: Electrostatic Propulsion*, p. 237-250, Academic Press, New York, 1961.

[7] Mirels, H. "On Ion Rocket Neutralization." *Progress in Astronautics and Rocketry Volume 5: Electrostatic Propulsion*, p.373-381, Academic Press, New York, 1961.

[8] Buneman, O. and Kooyers, G. "Computer Simulation of the Electron Mixing Mechanism in Ion Propulsion." *AIAA Journal*, Vol. 1, No. 11, p.2525-2528, November 1963.

[9] Wadhwa, R.P. et al. "Two-Dimensional Computer Experiments on Ion-Beam Neutralization." *AIAA Journal*, Vol. 3, No. 6, p.1076-1081, June 1965.

[10] Tajmar, M. and Wang, J. "Three-Dimensional Numerical Simulation of Field-Emission-Electric-Propulsion Neutralization." *Journal of Propulsion and Power*, Vol. 16, No. 3, p.536-544, May 2000.

[11] Tajmar, M. and Wang, J. "Three-Dimensional Numerical Simulation of Field-Emission-Electric-Propulsion Backflow Contamination." *Journal of Spacecraft and Rockets*, Vol. 38, No. 1, p.69-78, January 2001.

[12] Pawlik, E.V. "Neutralization of a Movable Ion Thruster Exhaust Beam." *JPL Space Programs Summary 37-58*, Vol. III, 1969.

[13] Wang, et al. "Three-Dimensional Particle Simulations of Ion Propulsion Plasma Environment Deep Space 1." *Journal of Spacecraft and Rockets*, Vol. 38, No. 3, May 2001.
[14] Othmer, C. et al. "Three-dimensional simulations of ion thruster beam neutralization." *Physics of Plasmas*, Vol. 7, No. 12, p.5242-5251, Dec. 2000.
[15] Othmer, C. et al. "Numerical Simulation of Ion Thruster-Induced Plasma Dynamics – The Model and Initial Results." *Advances in Space Research,* Vol. 29, No. 9, p.1357-1362, Elsevier Science Ltd., UK, 2002.
[16] Othmer, C. et al. "Numerical Parameter Studies of Ion-Thruster-Beam Neutralization" *Journal of Propulsion and Power*, Vol 19, No. 5, p.953-963, September-October 2003.
[17] Kaganovich, I.D. et al. "Nonlinear charge and current neutralization of an ion beam pulse in a pre-formed plasma." *Physics of Plasmas*, Vol. 8, No. 9, September 2001.
[18] Wheelock, A., Gatsonis, N., and Cooke, D. "Ion Beam Neutralizatin Processes for Electric Micropropulsion Applications" AIAA-2003-5148, 39th Joint Propulsion Conference and Exhibit, Huntsville, AL July 20-23 2003.
[19] Wheelock, A., Cooke, D. and Gatsonis, N. "Computational Modeling of Ion Beam-Neutralizer Interactions in Two and Three Dimensions." AIAA-2004-4121, 40th Joint Propulsion Conference and Exhibit, Ft. Lauderdale, FL July 11-14 2004.
[20] Watson, D. F., "Computing the Delaunay Tessellation with Application to Voronoi Prototypes," *The Computer Journal*, Vol. 24(2), pp. 167-172, 1981.
[21] Baker, T. J., "Automatic Mesh Generation for Complex Three-Dimensional Regions Using a Constrained Delaunay Triangulation," *Engineering with Computers*, Springer-Verlag, No. 5, pp.161-175, 1989.
[22] Birdsall, C.K., A. B. Langdon, "Plasma Physics via Computer Simulations", *Plasma Physics Series*, 1991.
[23] Bird, G.A. *Molecular Gas Dynamics and the Direct Simulation of Gas Flows,* Clarendon Press, Oxford, 1994.
[24] Boris, J.P., "Relativistic Plasma Simulation-Optimization of a Hybrid Code", Proceedings of the Fourth Conference on Numerical Simulation of Plasma, Naval Res. Lab, Washington D.C., 3-67, 2-3 November, 1970.
[25] Balay, S., Gropp, W., McInnes, L., and Smith, B. "Efficient Management of Parallelism in Object Oriented Numerical Software Libraries." In *Modern Software Tools in Scientific Computing*, ed. Arge, E. et al., pp. 163-202. Birkhauser Press, 1997.
[26] Saad, Y. and Schultz, M. "GMRES: A generalized minimal residual algorithm for solving nonsymmetric linear systems." *SIAM J. Sci. Statist. Comput.* 7:856-869, 1986.